

2019

HIV-1 entry in renal tubule epithelial cells through HSPG-dependent uptake pathways

<https://hdl.handle.net/2144/36299>

"Downloaded from OpenBU. Boston University's institutional repository."

BOSTON UNIVERSITY
SCHOOL OF MEDICINE

Thesis

**HIV-1 ENTRY IN RENAL TUBULE EPITHELIAL CELLS THROUGH HSPG-
DEPENDENT UPTAKE PATHWAYS**

by

NAUSHIN S. ALI

B.Sc., University of Toronto, 2014

Submitted in partial fulfillment of the
requirements for the degree of
Master of Science

2019

© 2019 by
NAUSHIN S. ALI
All rights reserved

Approved by

First Reader

Karen Symes, Ph.D.
Associate Professor of Biochemistry

Second Reader

Benjamin K. Chen, M.D., Ph.D.
Professor of Infectious Diseases
Icahn School of Medicine at Mount Sinai

Third Reader

Ping Chen, Ph.D.
Assistant Professor of Infectious Diseases
Icahn School of Medicine at Mount Sinai

ACKNOWLEDGMENTS

I am indebted to Prof. Benjamin Chen for giving me the opportunity to work alongside his wonderful team over the past few years. I thank him and Ping Chen for their steady patience and guidance, especially through the several months it took to get the knockout cell lines to work! I am appreciative of the rest of the Chen lab for always being there to answer my questions and provide advice on experimental designs, even on weekends and holidays. The same goes for my advisor, Dr. Karen Symes, and MAMS director, Dr. Gwynneth Offner, who have continued to support my goals and helped me navigate every hoop I had to jump through to be here.

I am eternally grateful to my family and friends who supported me through this journey. It was not an easy sacrifice to be absent for almost 2 years, and I am thankful for those who continue to stand with me as I reach the finish line.

HIV-1 ENTRY IN RENAL TUBULE EPITHELIAL CELLS THROUGH HSPG-DEPENDENT UPTAKE PATHWAYS

NAUSHIN S. ALI

ABSTRACT

Human immunodeficiency virus (HIV) targets and depletes CD4⁺ T cells, compromising the body's ability to fight off infections. Progressed HIV disease can lead to impaired renal function known as HIV-associated nephropathy (HIVAN). Epithelial cells are typically ineffective targets of HIV-1 as they lack the CD4 and CCR5 molecules that are involved in viral entry into CD4⁺ T cells. However, previous research in the laboratory of Dr. Benjamin K. Chen demonstrated that renal tubule epithelial (RTE) cells were capable of viral uptake through a T cell-mediated, but CD4-independent mechanism. In addition, experiments implicated heparan sulfate proteoglycans (HSPG) as possible attachment receptors for HIV-1 through their heparan sulfate (HS) polysaccharide chains. The addition of anti-HSPG and anti-syndecan 1 antibodies blocked virus transfer by approximately 50%, suggesting a role for HSPG in viral entry. As a result, the syndecan (SDC) class of heparan sulfate receptors were assessed for their potential to serve as attachment receptors for HIV-1 through knockout studies. A co-culture system with donor HIV-expressing Jurkat T cells and target renal tubular epithelial (HK2) cells were used as a system for HIVAN pathogenesis and enabled cell-to-cell viral transfer. Despite the generation of stable SDC gene knockout lines, no change in viral transfer was observed, suggesting redundant or alternate pathways for HIV-1 entry. Understanding viral entry into epithelial cells is crucial as these sites can

serve as reservoirs for HIV-1, where it can continue to replicate even when plasma viral load has been sufficiently reduced with antiretroviral treatment.

TABLE OF CONTENTS

TITLE.....	i
COPYRIGHT PAGE.....	ii
READER APPROVAL PAGE.....	iii
ACKNOWLEDGMENTS	iv
ABSTRACT.....	v
TABLE OF CONTENTS.....	vii
LIST OF TABLES	ix
LIST OF FIGURES	x
LIST OF ABBREVIATIONS.....	xii
INTRODUCTION	1
HIV-Associated Nephropathy	1
Risk Factors	2
The Kidney as a Viral Reservoir	4
Cell-to-Cell HIV Transmission	6
Heparan Sulfate Proteoglycans	7
SPECIFIC AIMS	9
METHODS	10
RESULTS.....	15

Optimization of Jurkat to HK-2 HIV-1 Transfer	15
Design of Syndecan-Targeting CRISPR Constructs	17
Syndecan-1.....	20
Syndecan-2.....	22
Syndecan-3.....	25
Syndecan-4.....	28
DISCUSSION.....	32
Future directions.....	35
LIST OF JOURNAL ABBREVIATIONS	36
REFERENCES	37
CURRICULUM VITAE.....	39

LIST OF TABLES

Table 1: 20 base-pair (bp) guide sequences for SDC1.	18
Table 2: 20 bp guide sequences for SDC2.....	18
Table 3: 20 bp guide sequences for SDC3.....	19
Table 4: 20 bp guide sequences for SDC4.....	19
Table 5: 20 bp guide sequences for non-targeting control (scramble).....	19

LIST OF FIGURES

Figure	Title	Page
1	Interactions of various factors contributing to HIVAN, adapted from Cohen et al, 2017.	4
2	Co-culture system for assessing viral transfer.	13
3	Summary of experimental design.	14
4	Nucleofection of Jurkat cells with varying concentrations of HIV Gag-iGFP for use as donor cells in cell-to- cell transfer studies	15
5	Profile of GFP fluorescence in HK2 cells after co-culture with Jurkat cells transfected with varying concentrations of HIV Gag-iGFP	16
6	Normalized HIV-1 transfer efficiencies from Jurkat cells to HK2 cells	17
7	Percentage of SDC-1 expression in HK-2 cells at day 31 post-transduction	20
8	Jurkat to HK-2 HIV-1 transfer in SDC1(-) lines	21
9	Overview summary of SDC-1 experiments	22
10	Percentage of SDC-2 expression in HK-2 cells at day 16 post-transduction	23

11	Jurkat to HK-2 HIV-1 transfer in SDC2(-) lines	24
12	Overview summary of SDC-2 experiments	25
13	Percentage of SDC-3 expression in HK-2 cells at day 24 post-transduction	26
14	Jurkat to HK-2 HIV-1 transfer in SDC3(-) lines	27
15	Overview summary of SDC-3 experiments	28
16	Percentage of SDC-4 expression in HK-2 cells at day 22 post-transduction.	29
17	Jurkat to HK-2 HIV-1 transfer in SDC4(-) lines	30
18	Overview summary of SDC-4 experiments	31

LIST OF ABBREVIATIONS

ATCC.....	American Type Culture Collection
BSA.....	Bovine Serum Albumin
cART.....	Combined Antiretroviral Therapy
FBS	Fetal Bovine Serum
FSGS.....	Focal Segmental Glomerulosclerosis
GFP	Green Fluorescent Protein
HEK	Human Embryonic Kidney
HIV-1	Human Immunodeficiency Virus-1
HIVAN.....	HIV-Associated Nephropathy
HK-2	Human Kidney 2
HSPG	Heparan Sulfate Proteoglycan
PBMC	Peripheral Blood Mononuclear Cell
PBS	Phosphate Buffered Saline
PFA	Paraformaldehyde
RTE.....	Renal Tubule Epithelial
SDC.....	Syndecan
US	United States

INTRODUCTION

There are approximately 37 million individuals currently living with human immunodeficiency virus (HIV) worldwide [1-3]. Almost three-quarters of HIV-infected individuals reside in sub-Saharan Africa, where there is a higher prevalence of infection compared to the United States (US) [1, 3]. While the global rate of new HIV infection has decreased by 38% since 2001 [3], there were 2 million new cases of HIV infections that occurred in 2015 [1-3]. Currently, it is estimated that there are 1.2 million HIV-positive individuals in the United States, where the annual incidence has remained stable over the past decade at ~50,000 cases per year [1, 3]. Today, HIV infection can be described as a chronic illness with the advent of antiretroviral therapy, which suppresses viral replication [1].

HIV-Associated Nephropathy

Shortly after the HIV epidemic began in the early 1980s, renal dysfunction was recognized as a possible complication of progressed HIV disease [1, 3, 4]. In 1984, a landmark paper by Rao *et al* investigated the prevalence of kidney disease among HIV-infected individuals in the US [5]. They described the first cases of what is now known as HIV-associated nephropathy (HIVAN), which affects all renal compartments including the interstitium, glomeruli and tubules. Local HIV infection of the kidney precludes the diagnosis of HIVAN, with the virus infecting podocytes as well as tubular- and glomerular epithelial cells.

Clinically, HIVAN presents with proteinuria, impaired renal function and occasionally edema [1, 3]. Some patients may also be edematous due to malnutrition and/or salt wasting caused by renal tubular injury. Histologically, HIVAN is described as a distinct form of collapsing focal segmental glomerulosclerosis (FSGS). As expected, FSGS is characterized by segmental scarring of the glomeruli. Additional histological markers include interstitial inflammation, fibrosis, and microcystic renal tubular dilatation [1].

Before the introduction of combined antiretroviral therapy (cART), about 3-10% of HIV-infected individuals in the US were diagnosed with HIVAN [1]. Following widespread use of cART, the incidence of HIVAN has since decreased [1]. In the absence of cART, HIVAN rapidly progresses to end-stage renal disease (ESRD), causing significant kidney impairment that necessitates dialysis and eventually kidney transplant [1]. Given that patients having increasingly longer life expectancies with cART, the prevalence of ESRD continues to increase [1, 4].

Risk Factors

While the rates of HIVAN vary across the globe, the region with the highest prevalence is sub-Saharan Africa [1, 2, 4]. In the United States, HIVAN occurs more commonly in those of African descent, which can be partially attributed to genetic susceptibility [1, 4]. The onset of HIVAN in a given individual can further be illuminated by the interactions among pathogen, host, environmental and behavioral attributes [1], summarized in Figure 1. Specifically, environmental and behavioral factors include

access to and compliance with standard of care treatments including cART. Pathogen factors can include the variability in viral protein expression in the kidney. Host factors are in part characterized by genetic predispositions that largely affect patients of African descent [1, 4].

One such gene involved is *APOLI* which encodes apolipoprotein L1, a protein component of certain high-density lipoproteins that make up two types of trypanolytic factor, which confers protection against *Trypanosoma brucei*, the parasite that causes African sleeping sickness [1, 4]. Specific variants of *APOLI* have been shown to be strongly associated with HIVAN and are exclusively found in patients of African heritage, suggesting a positive selection. It is proposed that these “risk” alleles may confer an advantage through increased trypanolytic activity, not unlike the selective advantage of sickle-cell heterozygosity in regions where malaria is prevalent [1, 4].

Another gene enriched in African-American populations that has been strongly associated with HIV-associated FSGS in addition to idiopathic FSGS is *MHY9*, which codes for non-muscle myosin heavy chain IIA [4]. However, it is suggested that additional genetic and/or environmental factors are necessary to confer an increased risk of HIVAN [4].

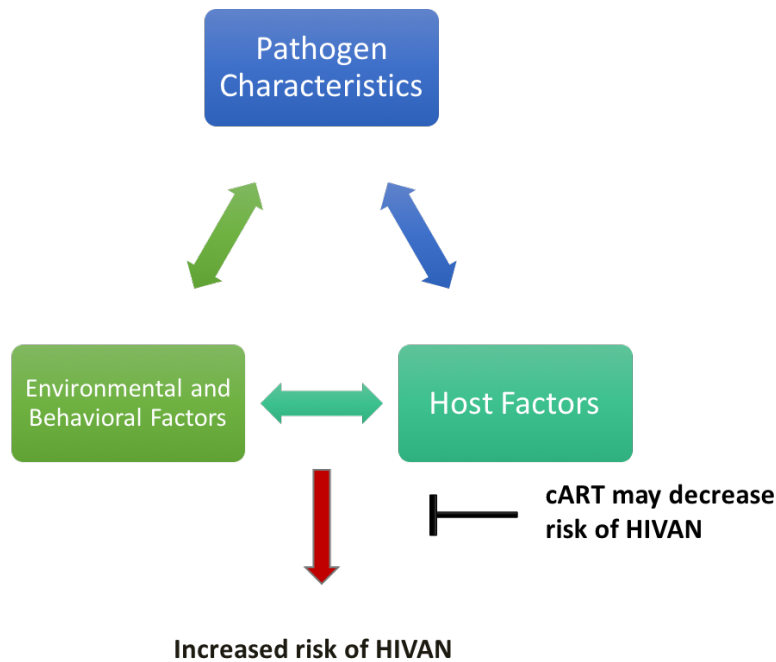


Figure 1: Interactions of various factors contributing to HIVAN, adapted from Cohen *et al*, 2017.

The Kidney as a Viral Reservoir

The pathogenesis of HIVAN was first described in 2000, when Bruggeman *et al* detected HIV-1 in renal tubule epithelial cells and glomerular podocytes, identifying a connection between HIV-1 and renal tissue [6]. They reported evidence that three of the four patients studied who had undetectable viral loads in circulation continued to have viral replication in renal compartments even on cART, suggesting the kidney may be a viral reservoir. *In situ* hybridization experiments performed on human kidney tissue showed the presence of both spliced and unspliced viral mRNA in these renal compartments.

Further evidence that the kidney could support viral infection was in a report by Winston *et al* who detected viral RNA intracellular expression in both the presence and absence of cART [7]. DNA extracted from renal biopsies before and after cART had clearly demonstrated that treatment had blocked further infection of kidney cells through the lack of the circular form of viral DNA containing long-terminal repeats, which are considered to be indicative of recent infection.

Elegant phylogenetic analyses of two patient kidney biopsies showed that HIV-1 viral variants from renal tubules clustered separately from those coming from PBMCs from each patient [8]. The discovery of unique renal viral variants was strongly suggestive that the kidney may serve as an independent site of replication.

Canaud *et al* assessed biopsies from HIV patients who underwent kidney transplants and found that both viral RNA and DNA were still present in podocytes and renal tubule epithelial cells [9]. This further strengthened the idea that viral replication continues in renal tissue despite systemic virological suppression on cART.

In 2014, Blasi *et al* were the first to demonstrate productive HIV-1 infection of renal tubule epithelial cells using immortalized and primary cell lines [10]. That is, following viral transfer to renal cells, HIV-1 was reverse-transcribed and integrated into the target genome. These infected renal cells were able to produce new virus particles and transfer them back to T cells in a contact-dependent manner. These findings, along with those described earlier, supported the notion that the kidney acts as an HIV-1 reservoir.

Cell-to-Cell HIV Transmission

The first study to explore entry mechanisms into epithelial cells found that under *in vitro* conditions, cell-to-cell infection mediated by T cells was significantly more efficient than transmission through cell-free virus [11]. The presence of infiltrating T cells in kidney biopsies of HIVAN patients further supported the notion that T lymphocytes may play a direct role in transferring HIV-1 to renal tissue [6].

The two typical pathways that are known to facilitate viral entry, via membrane fusion or endocytosis into a cell, are both receptor-mediated. Yet epithelial cells lack the CD4 and CCR5 receptors that are classically involved in viral entry into CD4⁺ T cells, which would suggest that they are ineffective targets [10, 11]. This led to a search by several investigators for molecules that mediate HIV-1 entry into renal epithelial cells. While one study found that the C-type lectin receptor, DEC-205, appeared to facilitate T-cell dependent HIV-1 entry into the immortalized renal tubule epithelial cell line HK2, there was no evidence of a productive infection [12].

Recently, an *in vitro* system co-culture system was used by Chen *et al* to further characterize cell-to-cell HIV-1 transfer [13]. Briefly, HIV-infected Jurkat T cells were co-cultured with uninfected HK2 cells and found to produce a more robust infection than cell-free virus infection of HK2 cells. This viral entry mechanism was determined to be CD4- and Env-independent. Furthermore, chemical inhibitors of heparan sulfate proteoglycans (HSPGs) as well as monoclonal antibodies targeting HSPG, Syndecan-1 and agrin all showed a significant reduction (~50%) in cell-to-cell virus transfer. Given that heparan sulfates have been known to play a role in cell adhesion, it was hypothesized

that the inhibitors used may affect cell-cell contact and suggest a specific role of these molecule subtypes in HIV-1 entry in renal epithelial cells.

Other groups have also found HSPG involvement in HIV-1 transmission from T cells to intestinal epithelial cells (HT29), which further support nonconventional cell surface HIV-1 entry pathways through what Alfsen *et al* termed a “viral synapse” [14].

Heparan Sulfate Proteoglycans

HSPGs comprise a large class of proteins that contain HS glycosaminoglycan (GAG) polysaccharide chains [15]. Heparan sulfates are conjugated to different types of proteins that each have preferential localizations. For example, perlecan is distributed on the extracellular matrix, and both glipicans and syndecans are associated with the cell surface. The canonical model of the role of HSPGs in endocytosis had long described ligand binding to HSPG that resulted in a ligand-specific conformational change which enabled ligand presentation to endocytic receptors. Endocytosis further can be divided into clathrin- dependent and independent internalization; both pathways may be used in SDC- and glipican-mediated entry.

Syndecans (SDCs) are a type I transmembrane HSPG that have an extended extracellular domain that contains three heparan sulfate chains [15, 16]. Syndecans interact with ligands through the sulfated regions of the HS chains and the basic amino acid residues on the ligand’s surface. There are 4 members of the SDC family: SDC-1, SDC-2, SDC-3, and SDC-4. While the former has been shown to be the primary syndecan expressed on epithelial surfaces, the other three have still been shown to be expressed at varying levels depending on tissue-type.

In one study by Bobardt *et al*, each syndecan subtype was introduced to B lymphocytes that natively lack HIV-1 attachment receptors such as CD4, lectins and HSPGs and was shown to facilitate HIV-1 entry [17]. When the heparan sulfate chains were enzymatically cleaved, HIV-1 entry was inhibited, signifying that these chains contain the HIV-1 binding sites on the target cell.

These syndecan subtypes remain to be individually investigated in renal tubule epithelial cells for their potential role in viral entry, as suggested by Chen *et al* [13].

SPECIFIC AIMS

Previous research at the laboratory of Dr. Benjamin K. Chen demonstrated that renal tubule epithelial (RTE) cells were capable of viral uptake through a T cell-mediated, but CD4-independent mechanism [13]. In addition, the studies supported the hypothesis that heparan sulfate proteoglycans (HSPGs) can serve as attachment receptors for HIV through their heparan sulfate (HS) polysaccharide chains. The addition of anti-Syndecan 1 antibodies blocked virus transfer by approximately 50%, suggesting a role for the syndecan family in viral entry.

Understanding viral entry into epithelial cells is crucial as these sites can serve as reservoirs for HIV, where it can continue to replicate even when plasma viral load has been sufficiently reduced with antiretroviral treatment.

The goal of this study was to use inhibition assays to assess HIV-1 entry in renal tubule epithelial cells through cell-to-cell transfer. CRISPR/Cas9 gene editing technology was used to knock out and to assess importance of the syndecan (SDC) family as attachment receptors in viral transfer.

METHODS

Cells and Tissue Culture

The human renal proximal epithelial cell line HK-2 and CD4+ Jurkat T-cell line were obtained from American Type Culture Collection. Jurkat cells were maintained in RPMI 1640 (Gibco), with 100 U/mL penicillin, 100 µg/mL streptomycin, and 10% fetal bovine serum (FBS). Cells were passaged and maintained at a density of $<5 \times 10^5$ cells/mL. HK-2 cells were cultured in Keratinocyte-SFM (Invitrogen) supplemented with 2.5 mg/mL bovine pituitary extract and 0.25 g/mL recombinant EGF. The lentivirus-packaging cell line 293T (ATCC) was cultured in DMEM (Sigma-Aldrich) supplemented with 100 U/mL penicillin, 100 µg/mL streptomycin, and 10% FBS.

CRISPR Plasmid Construction

A lentiCRISPRv2-puromycin plasmid that was previously digested with *BsmBI* was used. Short guide RNAs (sgRNAs) targeting SDC-1, SDC-2, SDC-3, and SDC-4 genes were developed based on the protocols of Dr. Feng Zhang from MIT [18] and chosen based on minimizing off-target effects (Tables 1-4). Each target sequence was synthesized as a pair of oligonucleotides, treated with T4 polynucleotide kinase and then annealed in T4 DNA ligation buffer. The double-stranded oligos were diluted 1:100 and incubated with the lentiCRISPRv2-puromycin plasmids to set up a ligation reaction in presence of T4 DNA ligase. This mixture was transformed into Stbl2 competent cells (Invitrogen) under carbenicillin selection. Plasmids were then isolated by miniprep (Qiagen) and verified through DNA Sanger sequencing.

Lentivirus Production

293T cells were seeded in a 6-well format at $4-8 \times 10^5$ cells per well 18-24 hours prior to transfection. 30 minutes prior to transfection, 1mL of serum-containing media from each well was removed. Each transfection reaction consisted of a PolyJet-DNA complex in a 3:1 ratio created in a 96-well plate. The DNA complex was prepared by combining 0.5 μ g of envelope (VSV-G) plasmid, 1.0 μ g of packaging (PAX2) plasmid, and 1.5 μ g of vector (lentiCRISPRv2-puromycin targeting SDC-1, SDC-2, SDC-3, SDC-4 or a non-targeting control) plasmid. 293T cells were transfected according to the manufacturer's protocol (SignaGen). At 48 hours post-transfection, viral supernatants were harvested (~1.8 mL), filtered through a 0.22 μ m filter, and stored in a freezer at -20°C.

Generation of Stable SDC Knockout Cell Lines

HK2 cells were seeded in a 6-well format and grown under normal culture conditions until reaching 50-60% confluency. At day 0, cells were then transduced with lentiCRISPRv2-puromycin lentiviruses targeting either SDC-1, SDC-2, SDC-3, SDC-4 or a non-targeting control (scramble). At 24 hours post-transduction (day 1), culture dishes were replaced with full media. At 48 hours post-transduction (day 2), cells were selected with 2 μ g/mL of puromycin for up to two weeks and expanded as needed. The knockout efficiency was assessed around day 13 with flow cytometry.

Immunofluorescence Staining for Assessment of SDC knockouts

HK2 cells were dissociated using a non-enzymatic solution, Versene (Gibco) and washed with ice cold phosphate buffered saline (PBS) 1% bovine serum albumin (BSA). Cells were then centrifuged and re-suspended at a concentration of $1-5 \times 10^5$ cells/mL with 100 μ L of a solution containing 1% BSA and a 1:500 dilution of an aqua live/dead stain (Invitrogen) in PBS. 5 μ L of an anti-hSyndecan APC-conjugated antibody specific for either SDC-1, SDC-2, SDC-3, or SDC-4 (R&D Systems) were added to each well and incubated in the dark for 45 minutes at 4°C. Appropriate isotype controls from R&D Systems were also used for each antibody. Cells were then washed 3 times by centrifugation at 300 g for 5 minutes and re-suspended in 500 μ L of ice cold PBS with 1% BSA. After the third wash, cells are fixed in 1% paraformaldehyde (PFA) and stored at 4°C until analysis by flow cytometry. The measure of SDC expression was assessed with FlowJo software.

HIV infection and Nucleofection of Donor T Cells

HIV-expressing donor cells were obtained by transfecting Jurkat cells with HIV-1 proviral constructs (HIV Gag-iGFP) using Amaxa nucleofection (Amaxa Biosystems). HIV Gag-iGFP expression was then assessed with flow cytometry. First, 6 μ g of HIV-1 proviral plasmids were nucleofected into 7×10^6 cells by using Amaxa Cell Line Nucleofector Kit V and Program S-18. Nucleofected Jurkat cells were enriched 24 hours later by centrifugation on a Ficoll density gradient. The enriched cells were cultured for an additional 24 hours before being used as donors in transfer experiments.

HIV-1 Cell-to-Cell Transfer

Jurkat to HK2 HIV-1 transfer was assessed in a co-culture system (Figure 2). The target HK2 cells were labelled with 2 μ M of CellTracker orange CMTMR fluorescent dye (Molecular Probes) for 30 minutes at 37°C and then washed with PBS. The labelled HK2 cells were seeded in a 24-well plate at 2.5×10^5 per well and cultured overnight. The following day, 1×10^6 donor Jurkat cells were added to the HK2 epithelial monolayer, and co-cultured for 4 hours. Termination of co-culture was completed by three PBS washes in order to remove Jurkat cells. The adherent HK2 cells were detached with 0.05% trypsin-EDTA, washed once, and then fixed with 1% PFA in preparation for analysis by flow cytometry. The measure of virus (HIV Gag-iGFP) transfer was assessed with FlowJo software. A summary of the experimental design from SDC knockout to assessing its relationship with viral transfer can be seen in Figure 3.

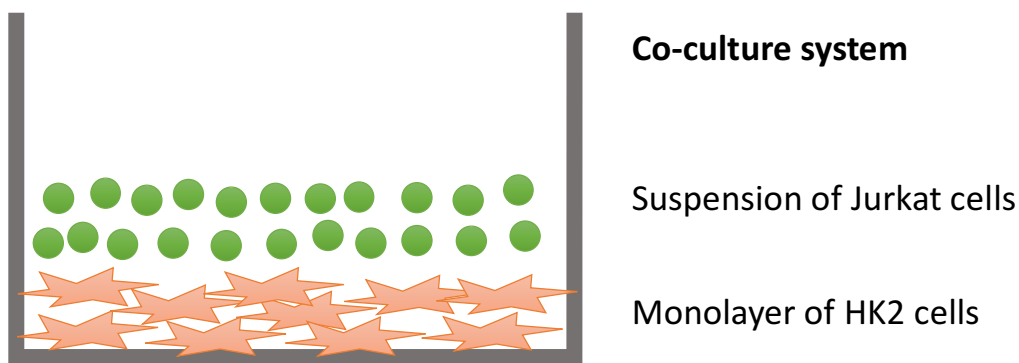


Figure 2: Co-culture system for assessing viral transfer.

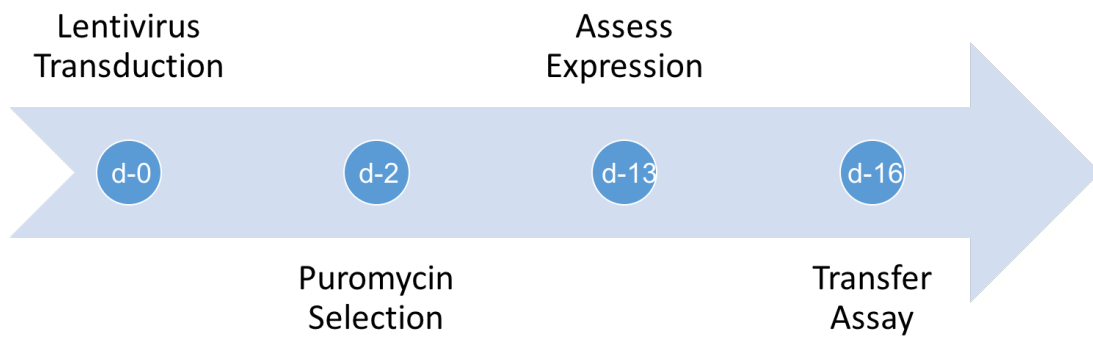


Figure 3: Summary of experimental design.

RESULTS

Optimization of Jurkat to HK-2 HIV-1 Transfer

In order to maximize the efficiency of HIV-1 introduction into Jurkat cells, 4 different HIV Gag-iGFP concentrations (4 μg , 6 μg , 8 μg , and 10 μg) were assessed for their nucleofection efficiency as well as for cell death (Figure 4). Given that GFP has been inserted into this proviral construct, viral particles can be visualized under light microscopy (Figure 4b). Virus uptake was assessed with flow cytometry.

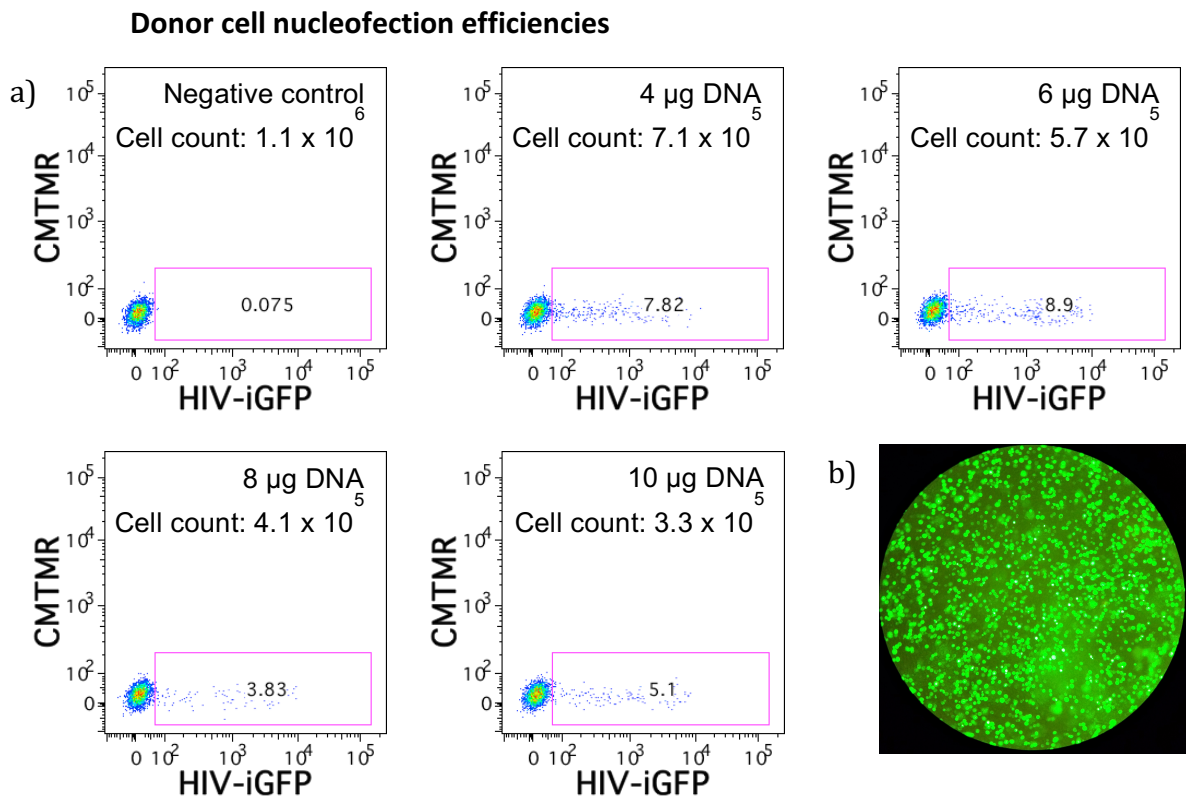


Figure 4: Nucleofection of Jurkat cells with varying concentrations of HIV Gag-iGFP for use as donor cells in cell-to-cell transfer studies. a) FACS profile of GFP fluorescence in Jurkat cells. b) Jurkat cells examined under light microscopy show punctate dots of GFP in the cytoplasm.

While the highest transfection occurred with 6 μg of HIV Gag-iGFP at 8.9% of the Jurkat cells being infected, the greatest cell survival in the infected populations was with 4 μg of Gag-iGFP (Figure 4a).

The Jurkat populations transfected with varying HIV Gag-iGFP concentrations were then co-cultured with target wild-type HK2 cells to assess virus transfer (Figure 5). From the raw data, 6 μg of HIV Gag-iGFP produced the highest transfer to HK2 cells at 13.3%. However, given the varying degree of cell death associated with Jurkat transfection, these transfer values were normalized to the control population to provide a more accurate comparison (Figure 6).

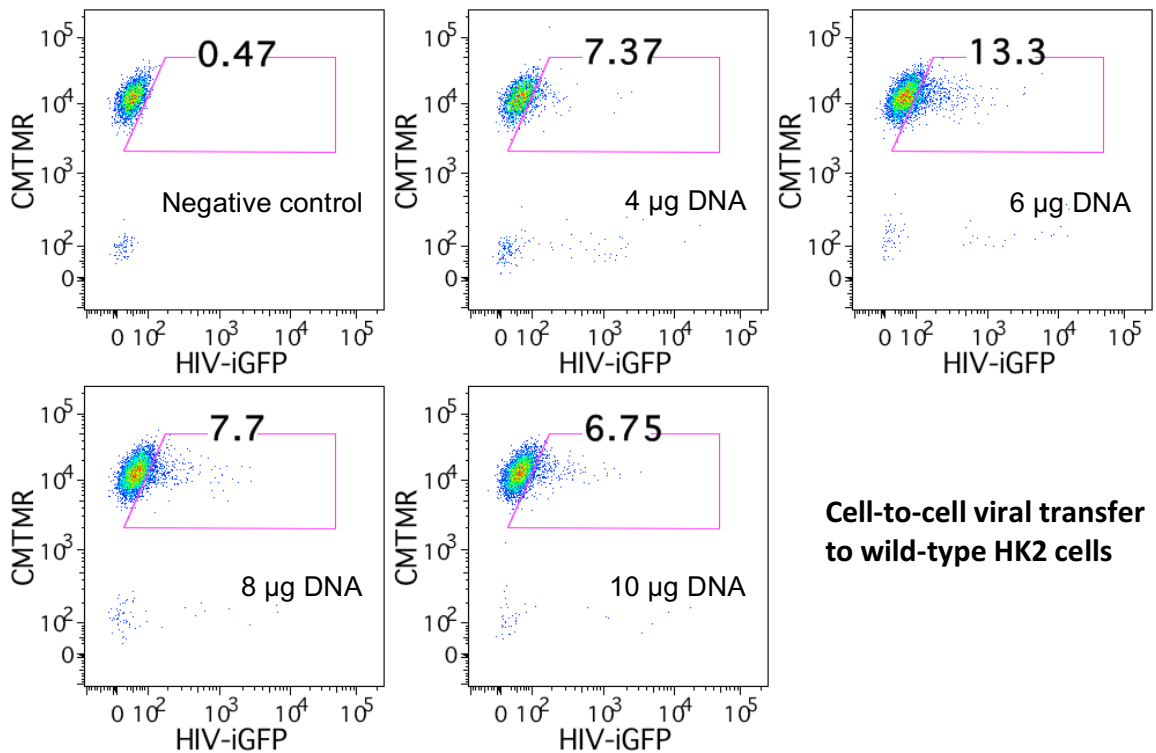


Figure 5: Profile of GFP fluorescence in HK2 cells after co-culture with Jurkat cells transfected with varying concentrations of HIV Gag-iGFP.

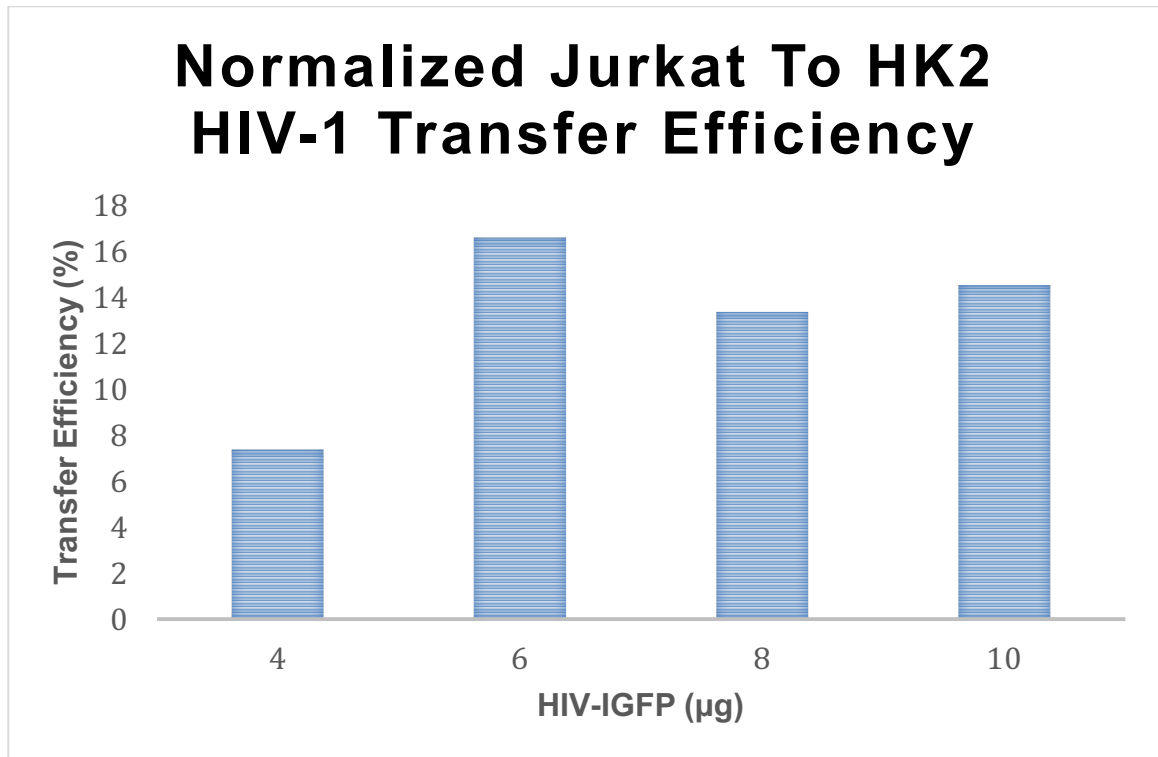


Figure 6: Normalized HIV-1 transfer efficiencies from Jurkat cells to HK2 cells. Jurkat cells were transfected with varying concentrations of HIV Gag-iGFP before used in transfer studies.

Following normalization of GFP expression among the different Jurkat populations, 6 µg of HIV Gag-iGFP still presented the highest virus transfer to HK2 cells in addition to having the highest transfection efficiency. For all subsequent co-culture transfer assays, 6 µg of HIV Gag-iGFP was used to transfect Jurkat cells.

Design of Syndecan-Targeting CRISPR Constructs

For each Syndecan subtype, 5-6 guide RNAs (gRNAs) were selected and 2 clones per target were extracted by miniprep were sequenced to verify construct insertion

(Tables 1-5). Clones that had a 100% match within the 20 bp gRNA sequence were combined. Final concentrations of minipreps ranged from 100-500 ng/ μ L.

Table 1: 20 base-pair (bp) guide sequences for SDC1.

Protein	Target	gRNA Sequence	20 bp match (%)
SDC1	1	TACAGCCGTATTCTCCCCCG	100
	2	GTTCCGGCGGTCAGGCTCCA	100
	3	CTTCTGGTAGGCCCCGCCGT	100
	4	ACAGCTCCCGACCACTCATC	n/a
	5	AGCCGAAACAAGCCAACGGC	100
	6	CCGGTGGGTTCTGGAGACGT	100

For SDC-1, target 4 gRNAs were not successfully inserted (as indicated in Table 1) into the lentiCRISPRv2-puromycin backbone and were discarded.

Table 2: 20 bp guide sequences for SDC2.

Protein	Target	gRNA Sequence	20 bp match (%)
SDC2	1	GATGACTACGCTTCTGCGTC	100
	2	GTTCTGTATATTCAGCGTCG	100
	3	GCGTAGTCATCGTCATCAAT	100
	4	TCATGCGATACACCAACAGC	100
	5	GGTCGAGATGTTGTCAGCTC	100
	6	TACGCATAAACTCCTTAGT	100

Table 3: 20 bp guide sequences for SDC3.

Protein	Target	gRNA Sequence	20 bp match (%)
SDC3	1	GTATGTGACGCTCGCCTGCT	100
	2	TGAGAACTTCGAGAGACCCG	100
	3	CCGAGCCCGACCCGAGTAG	n/a
	4	CTCTGGCTCATCCCGGATTG	100
	5	GCGCCGCCGATGAAGCCG	100
	6	AGCTGAGTGCCCGAGTCGA	100

Similarly, target 3 for SDC-3 was also not incorporated in miniprep and subsequently excluded from further experiments.

Table 4: 20 bp guide sequences for SDC4.

Protein	Target	gRNA Sequence	20 bp match (%)
SDC4	1	GCTTCACGCGTAGAACTCAT	100
	2	CGGAGCCCTACCAGACGATG	100
	3	CCCACTACATCCTCATCGTC	100
	4	CTCACCCGTTGAAGAGAGTG	100
	5	GCGTGCTGCTGTTCTTCGT	100

Table 5: 20 bp guide sequences for non-targeting control (scramble).

Protein	Target	gRNA Sequence	20 bp match (%)
Scramble	1	GTATTACTGATATTGGTGGG	100

Syndecan-1

Compared to the other syndecan subtypes, SDC-1 knockout lines were stable for the longest period of time, with expressions remaining low even at 31 days post-transduction (Figure 7). Targets 1, 2, and 6 had the lowest expression levels compared to wild-type and the scramble control.

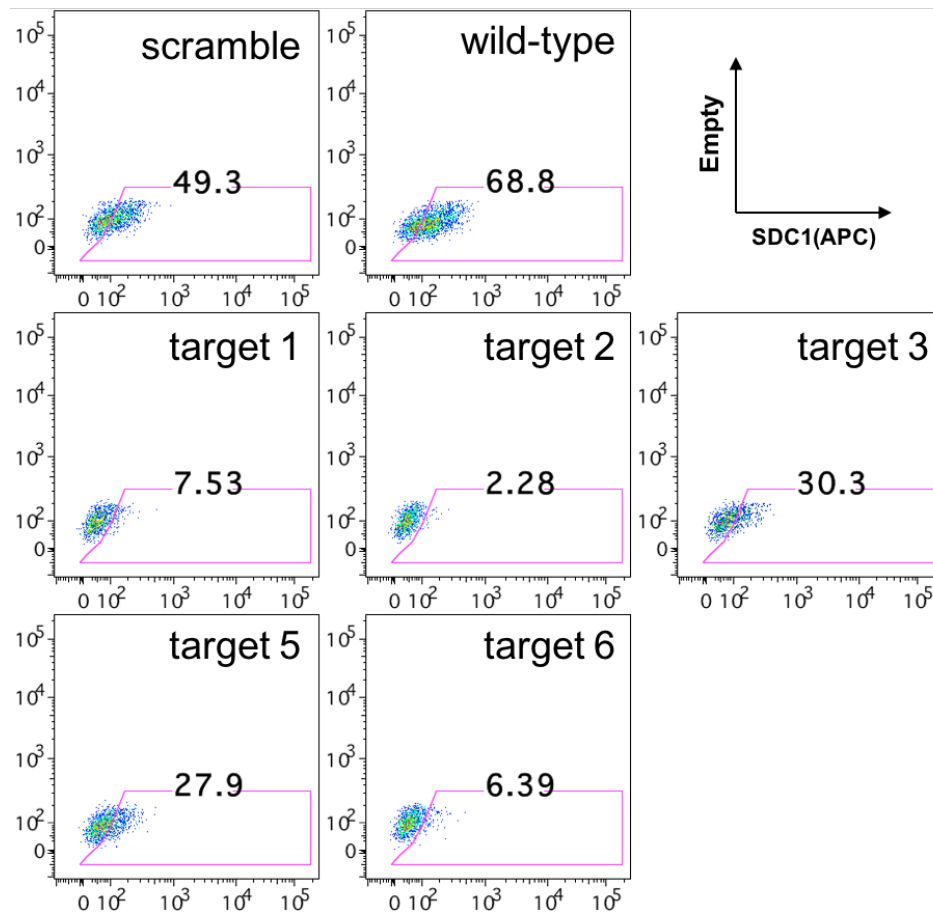


Figure 7: Percentage of SDC-1 expression in HK-2 cells at day 31 post-transduction.

A transfer assay was carried out 2 days after the SDC-1 staining to assess whether the knockout of SDC-1 would affect HIV Gag-iGFP virus transfer from Jurkat cells to HK-2 cells. Each condition was run in duplicates (not shown). As seen in Figure 8, no apparent change in virus transfer can be discerned between the knockout HK2 lines and the control (wild-type and scramble) HK2 populations.

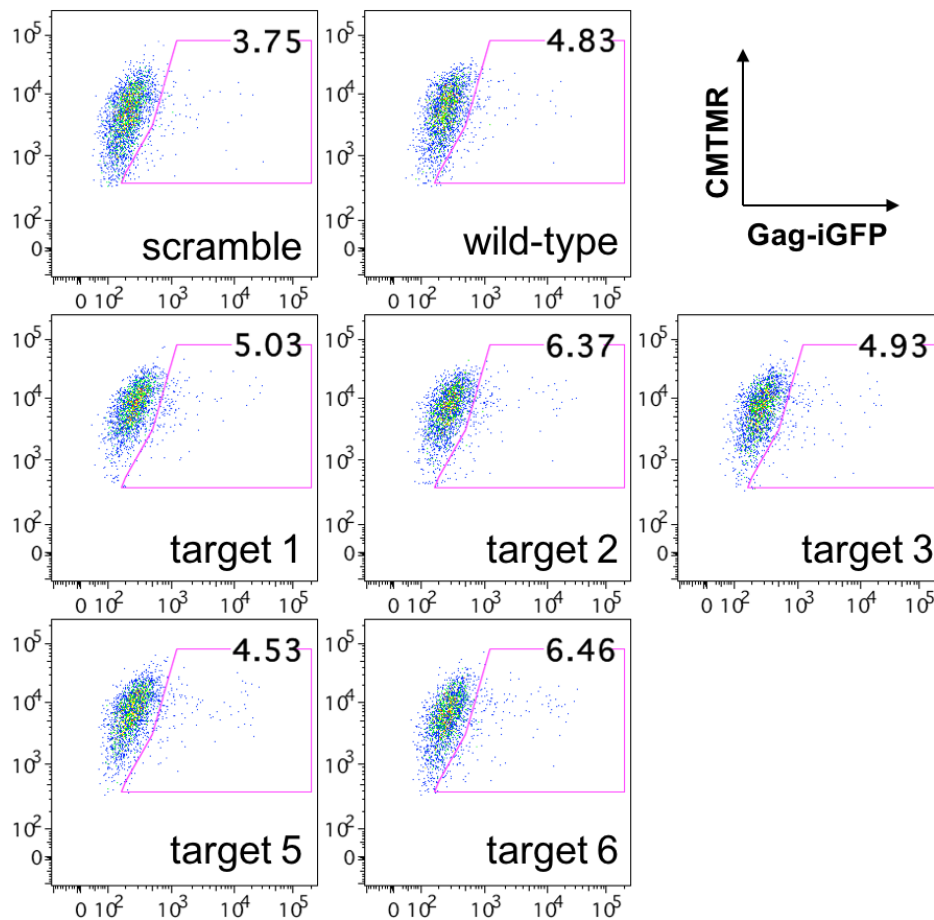


Figure 8: Jurkat to HK-2 HIV-1 transfer in SDC1(-) lines.

Syndecan expression was further plotted against HIV-1 virus uptake (Figure 9, lower panel). While there appears to be an inverse relationship with SDC1 expression and virus uptake, these results were not statistically significant.

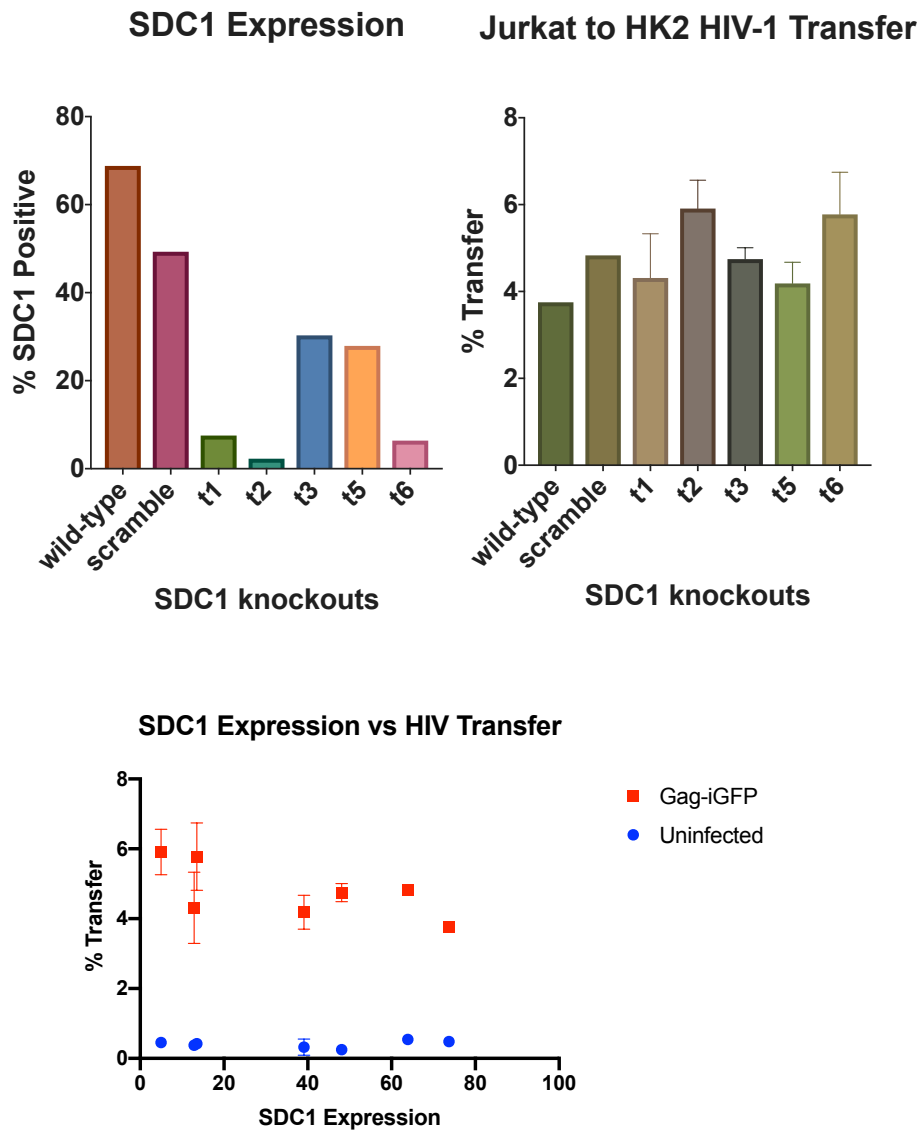


Figure 9: Overview summary of SDC-1 experiments.

Syndecan-2

SDC-2(-) lines did not display as robust reductions in target knockouts compared to wild-type (Figure 10). Moreover, SDC-2 wild-type expression has been shown to be consistently higher than SDC-1 expression (data not shown).

Furthermore, the knockout of SDC-2 was not as strong as SDC-1 knockouts, with a maximum of 35.6% reduction in SDC-2 surface expression (Figure 10). Knockouts, however, were assessed at later time points and found to show similar expression levels, implying that the variations in SDC-2 expression among these conditions are not due to stochastic variability (not shown).

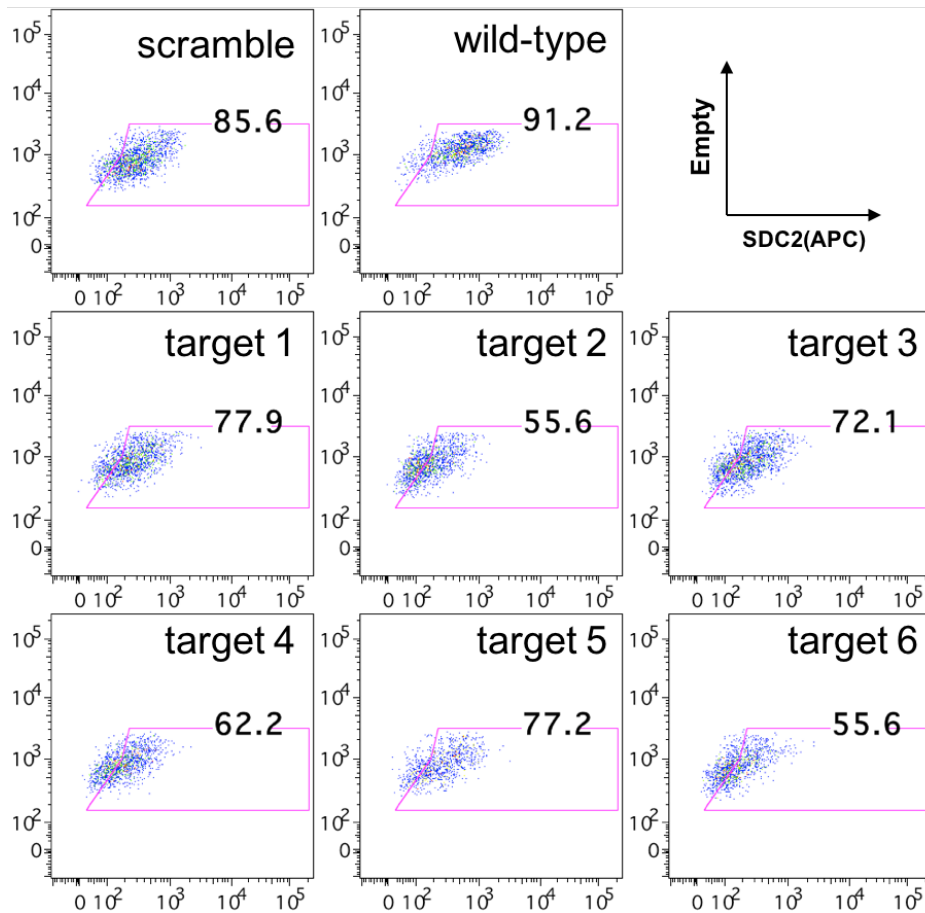


Figure 10: Percentage of SDC-2 expression in HK-2 cells at day 16 post-transduction.

The HK-2 cell lines with varying SDC-2 expression were then co-cultured with infected Jurkat cells to assess differences in virus uptake (Figure 11). While targets 2, 5,

and 6 appeared to have similar levels of virus uptake to wild-type and scramble-controlled HK-2 cells, there appeared to be a slight increase in virus uptake for targets 1, 2, and 4.

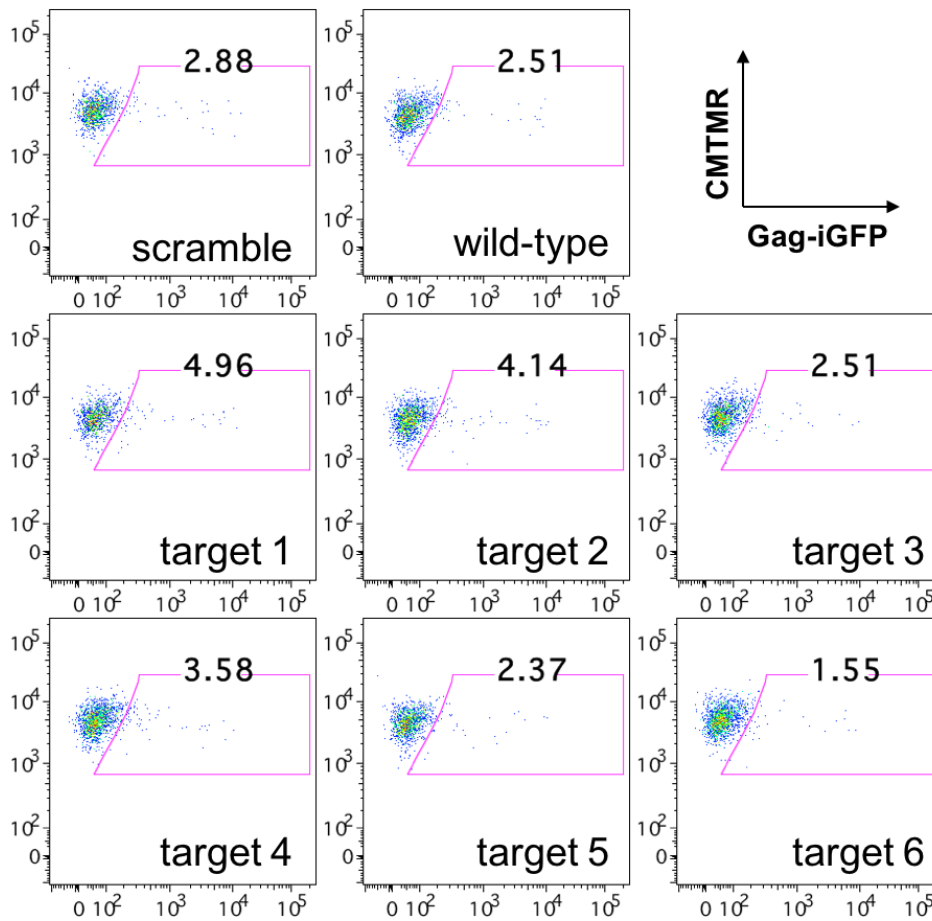


Figure 11: Jurkat to HK-2 HIV-1 transfer in SDC2(-) lines.

However, when comparing SDC-2 expression directly to virus uptake (Figure 12, lower panel), there is no discernable relationship that can be established.

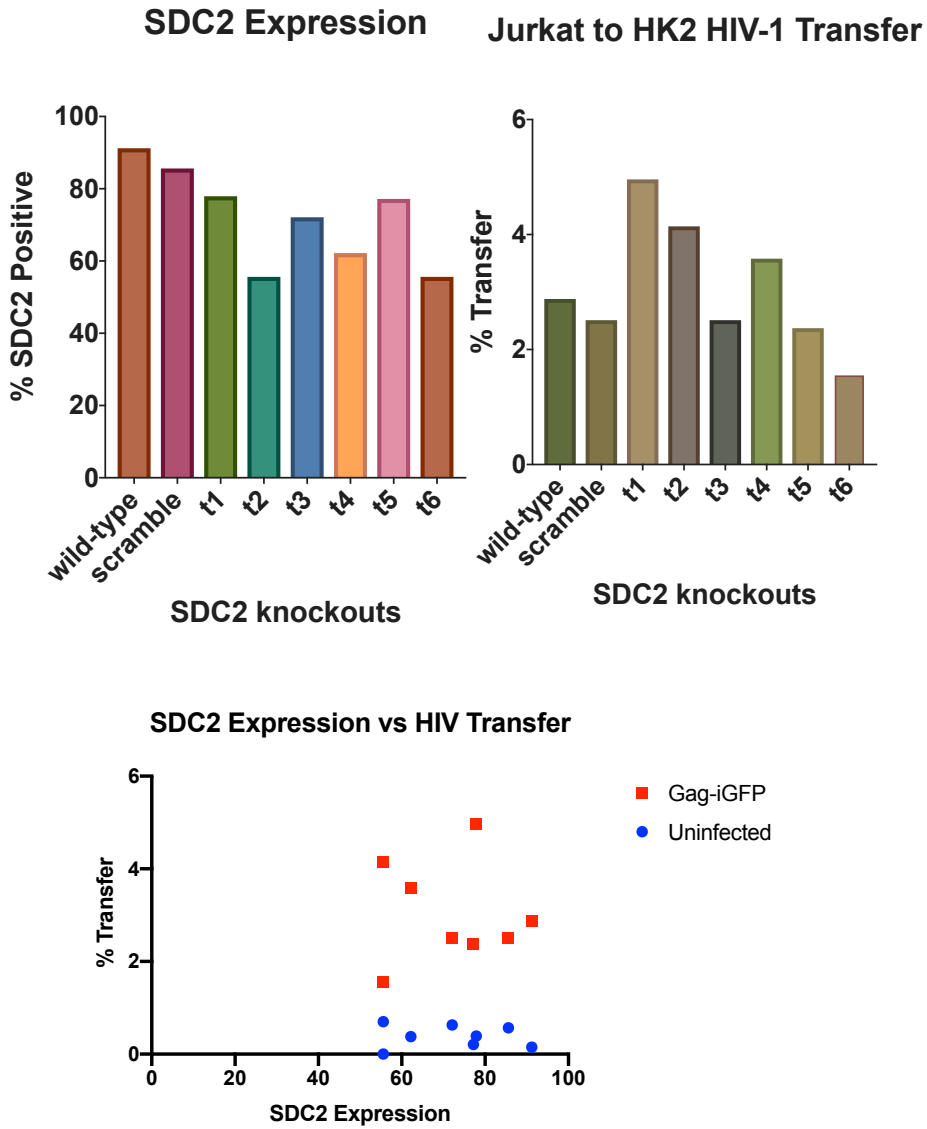


Figure 12: Overview summary of SDC-2 experiments.

Syndecan-3

At 24 days post-transduction, SDC-3 expression was assessed (Figure 13). Unlike the earlier two expression studies, there was a disparity in SDC-3 expression between the

wild-type and scramble-controlled HK-2 populations. Despite this significant deviation, a reduction in SDC-3 expression may still be concluded for targets 2, 4, 5, and 6.

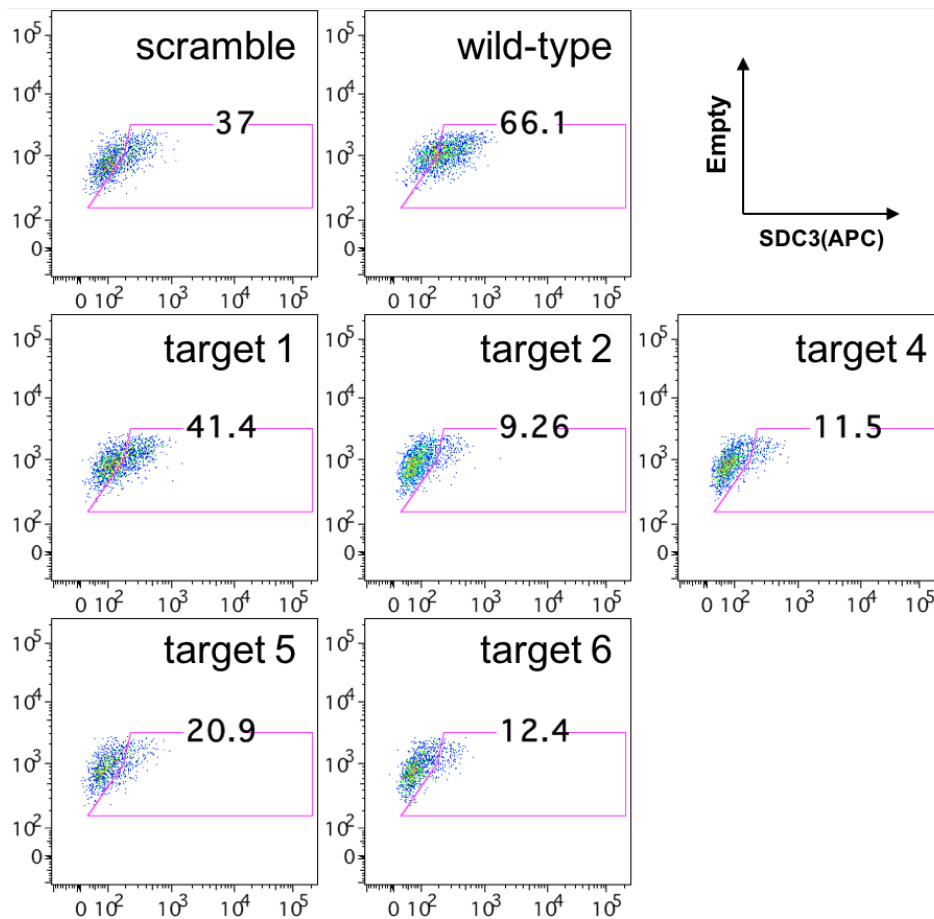


Figure 13: Percentage of SDC-3 expression in HK-2 cells at day 24 post-transduction.

When SDC-3(-) HK-2 cells were co-cultured with infected Jurkat cells, there was no difference in virus uptake regardless of SDC-3 expression levels (Figure 14).

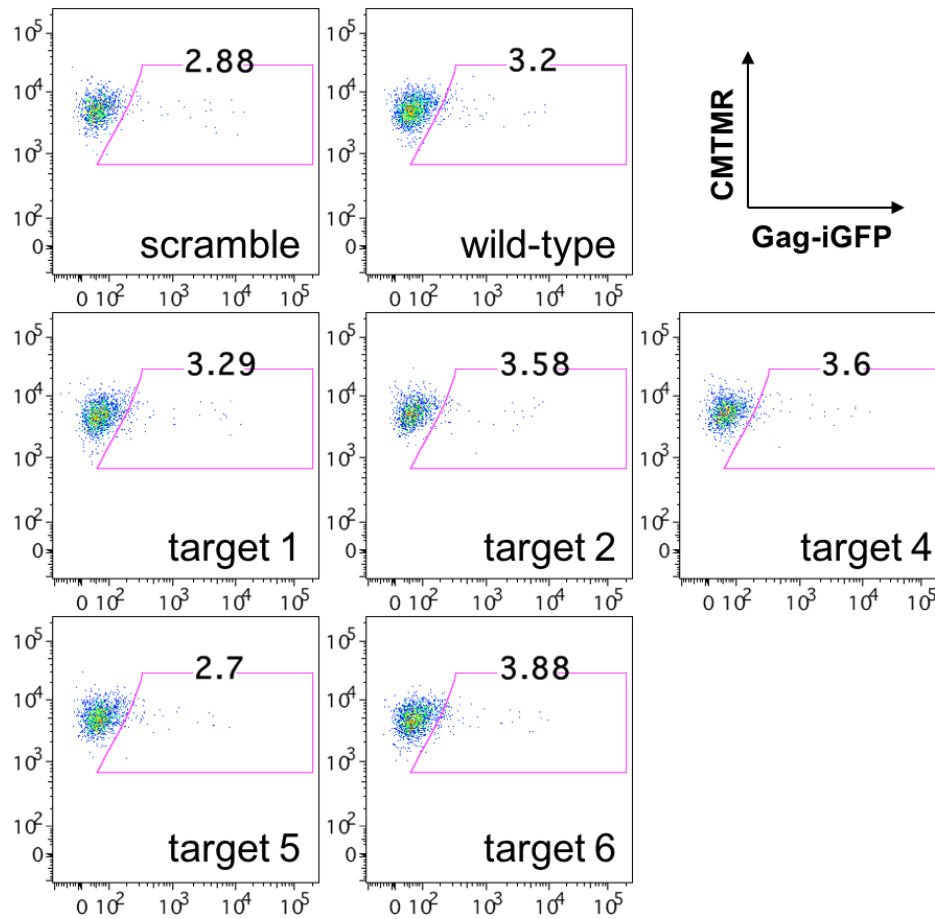


Figure 14: Jurkat to HK-2 HIV-1 transfer in SDC3(-) lines.

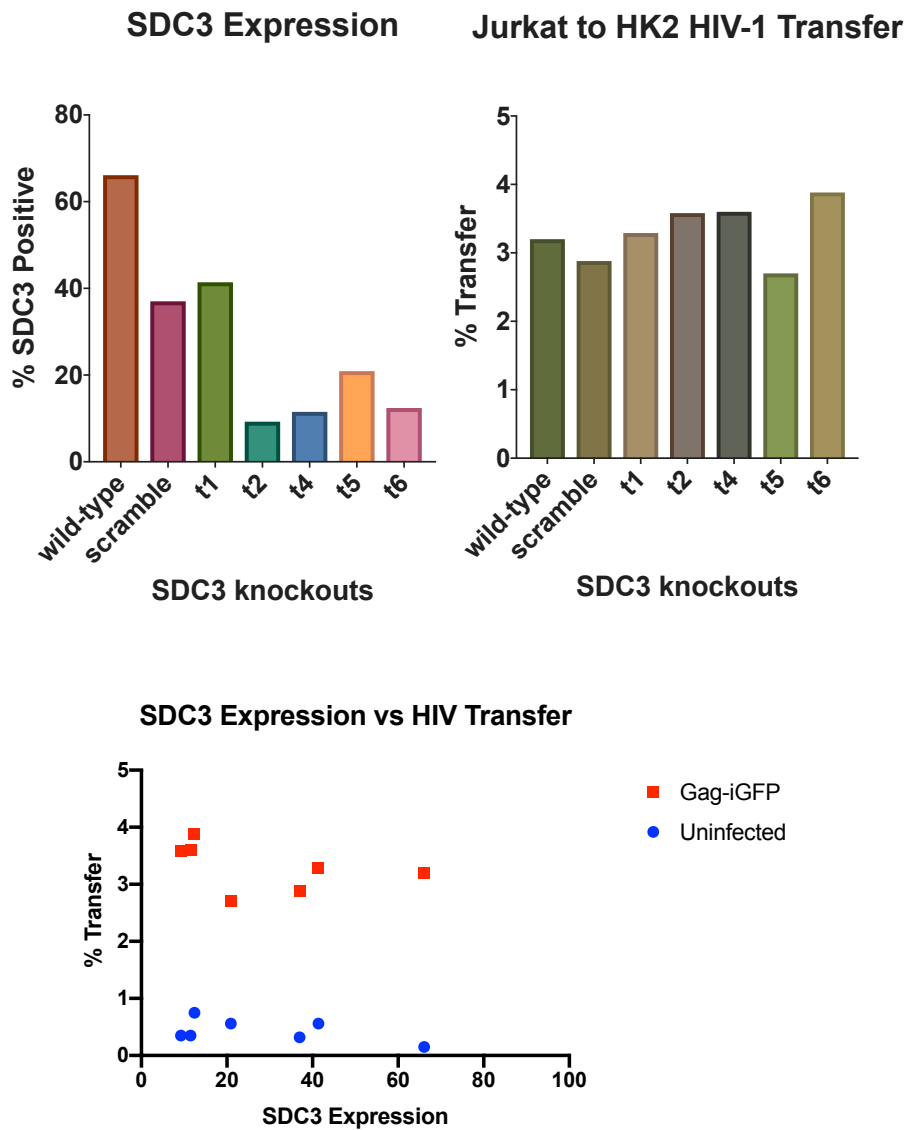


Figure 15: Overview summary of SDC-3 experiments.

Syndecan-4

SDC-4 expression levels in HK2 cells were assessed at 22 days post-transduction (Figure 16). Given the variation in SDC-4 expression between the wild-type HK-2 cells

and the scramble-controlled population, only targets 2-5 could be reliably concluded to produce a significant knockout effect.

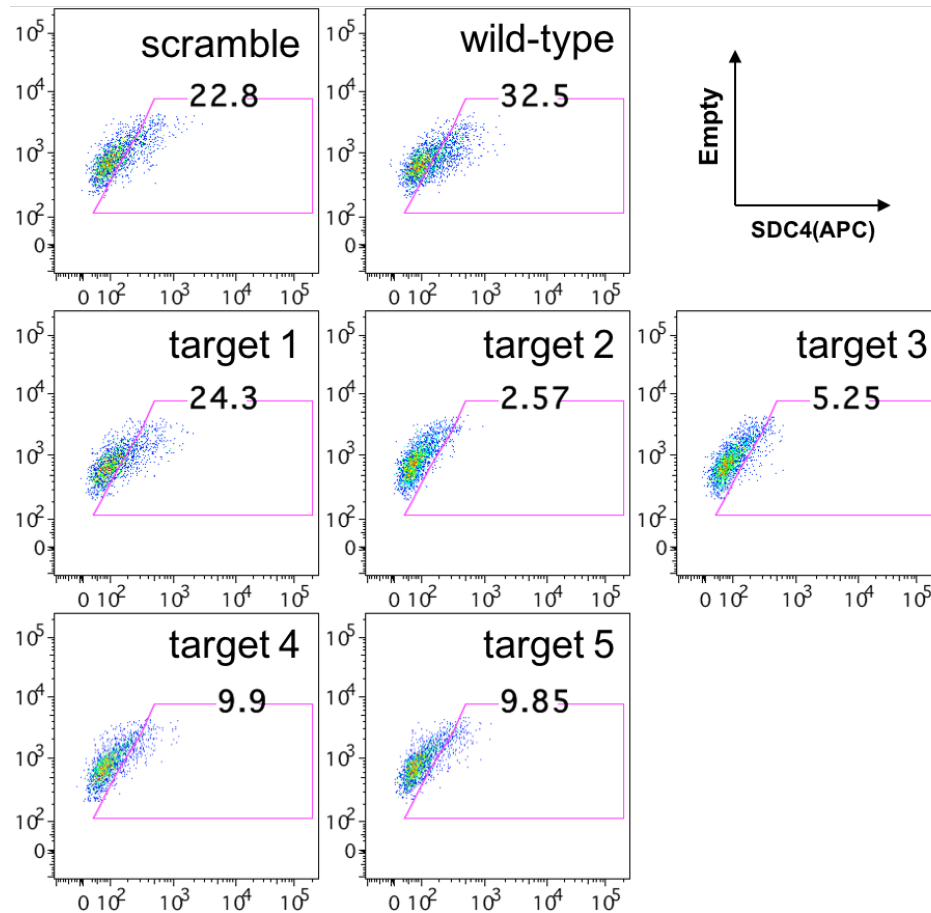


Figure 16: Percentage of SDC-4 expression in HK-2 cells at day 22 post-transduction.

In the co-culture assay for Jurkat to SDC4(-) HK-2 cells, little virus transfer could be seen in wild-type and knockout populations (Figure 17). Reactions have not been run with technical replicates or repeated, and so these results do not allow a conclusive determination as to whether SDC-4 expression levels affect virus uptake.

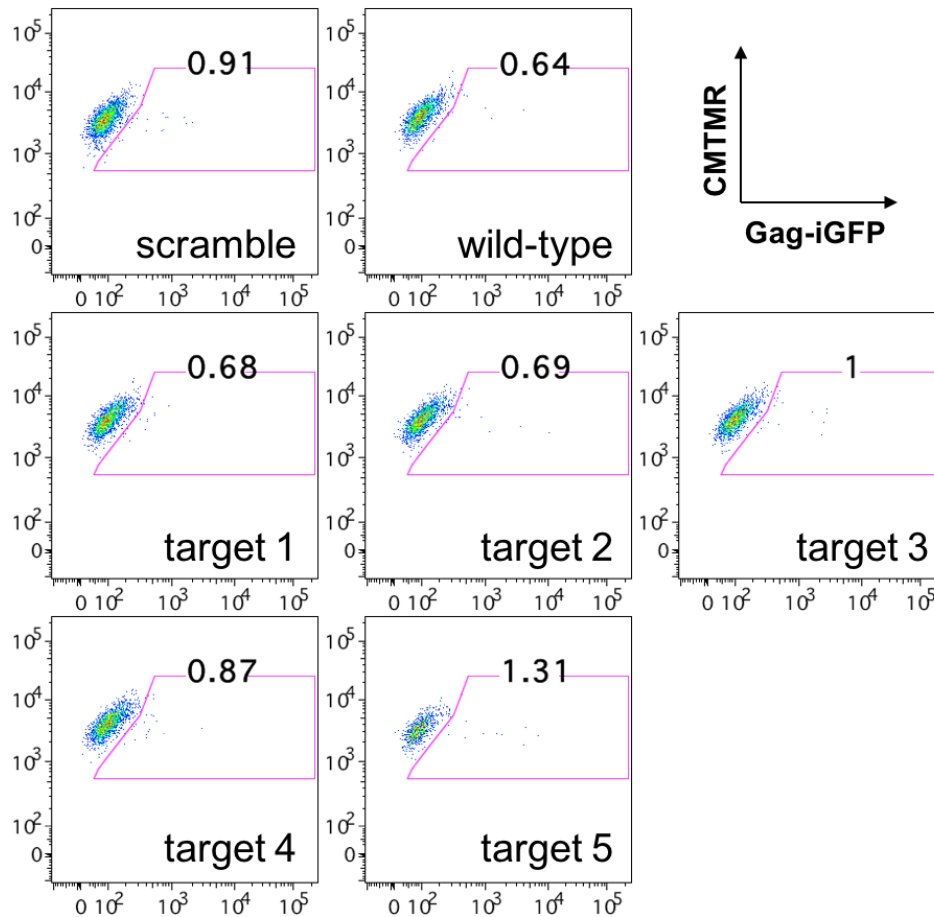


Figure 17: Jurkat to HK-2 HIV-1 transfer in SDC4(-) lines.

In this study we observed a poor overall cell-to-cell transfer efficiency, in the control cells, however, we still could detect some viral transfer and plotted SDC-4 expression against HIV-1 transfer to assess whether there may some impact of SDC-4 knockdown on cell-to-cell viral transfer (Figure 18).

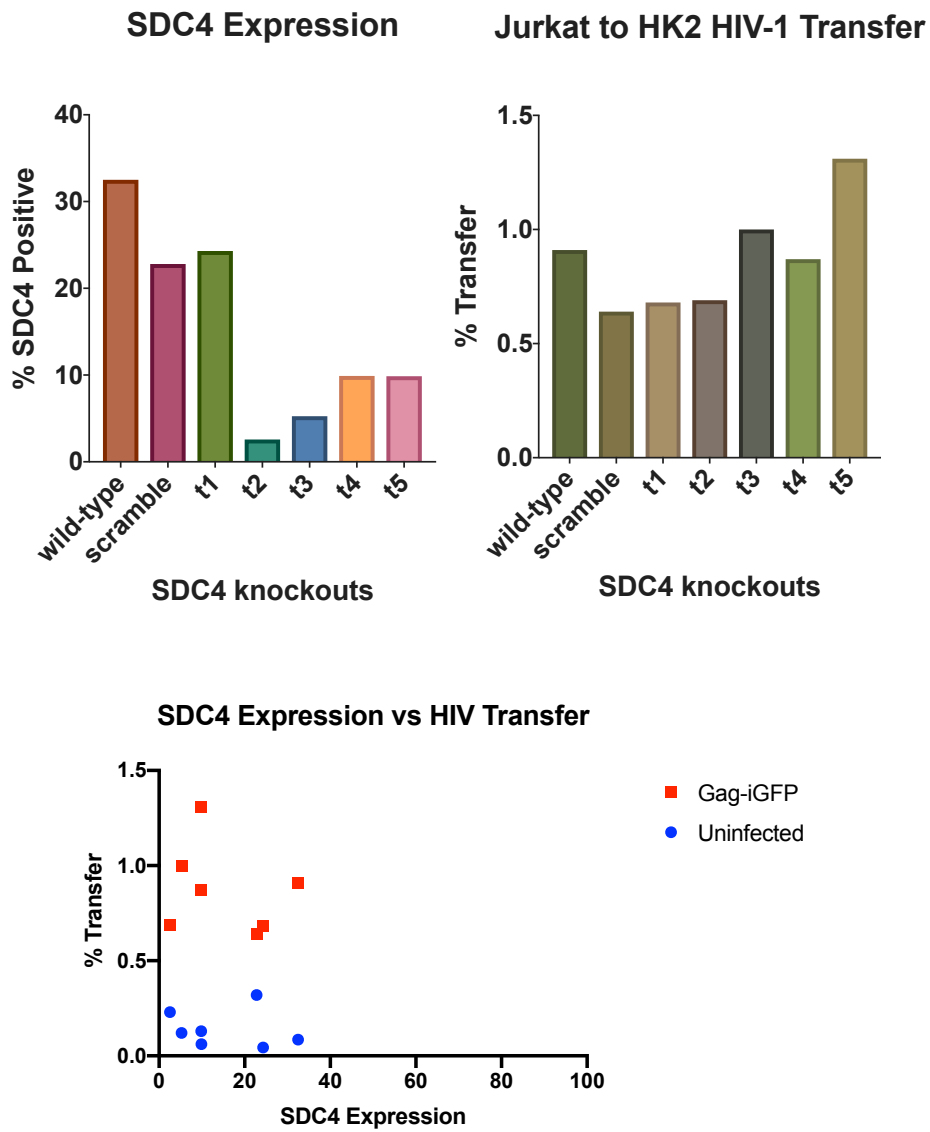


Figure 18: Overview summary of SDC-4 experiments.

DISCUSSION

The receptors involved in renal epithelial HIV-1 uptake have been evaluated by several laboratories [12, 13]. Despite the previous literature that suggests a role for HSPG receptors in cell-to-cell transfer, to-date, the members of this broad class of receptors have not been systemically assessed for their role. The purpose of this study was to elucidate whether members of the syndecan family may play a role in virus uptake mechanisms.

The immortalized human renal tubule epithelial cell line HK2 has previously been used as an *in vitro* system for studying HIVAN pathology [10, 13] and also used as donor cells in co-culture experiments to simulate cell-to-cell transfer. The modified molecular clone of HIV-1, Gag-iGFP, previously developed by the laboratory of Dr. Benjamin K. Chen and which was used in earlier work cited, was also chosen for this study for its validated capability in single-round infection, virus particle tracking, and quantification. This is due to the insertion of GFP between the matrix and capsid domains of the structural protein Gag, which oligomerizes at the plasma domain and facilitates infectious HIV-1 assembly [19, 20].

Through these experiments, it was observed that native HK2 cells expressed each syndecan subtype at varying levels, with SDC2 being the most prevalent and SDC4 being expressed at lower levels. The potential for variation the knockout efficiency of guide RNAs for each syndecan was considered, and 5-6 targets were chosen for each syndecan member. It was proposed that if a given syndecan subtype were involved, varying levels of that syndecan member would show a correlated change in viral transfer.

While previous work at our laboratory had shown a decrease in viral transmission when SDC-1 was blocked with monoclonal antibodies [13], there was no statistically relevant change in viral transfer to SDC1(-) HK2 cells. Similarly, there was no apparent change in viral transfer to HK2 cells that had decreased levels of expression of the other syndecan members (SDC2-4).

One caveat to consider is the phenomenon of syndecan shedding, which occurs through natural proteolytic processes but may also be induced by certain pathogens [15, 16]. This turnover process may affect syndecan-mediated ligand entry as soluble syndecans would compete with cell-surface syndecans, thus potentially masking ligand endocytosis and HIV-1 entry. Another potential drawback would be compensation of other syndecan or HSPG molecules in each knockout line, which could potentially mask minute changes in cell-to-cell viral entry. It may therefore be important to examine if the total HSPG expression is impacted by individual SDC knockouts and explore if combination knockouts may have a significant effect on viral transfer into the renal tubule cells. Finally, considering that the original HK2 cell population was heterogeneous, it is possible that cells in one well may have varying levels of knockout efficiencies which could not be parsed with this current experimental setup.

The primary issues that surrounded the study design were the experimental timeline, which necessitated knockout cell lines to be in culture for at least 2-3 weeks before they could be used for transfer studies. While there were usually enough cells for transfer by day 16 post-transduction, experiments were often run at a later date due to availability of Jurkat cells as donors as well as other time constraints. This was not

expected to pose any issue with regards to cell surface expression of the syndecans as it remained stable for at least three weeks, with varying levels of phenotype reversion after 30 days in culture (data not shown).

Another significant issue encountered was the inconsistent HIV Gag-iGFP transfection efficiencies of Jurkat cells, which have varied from 8 to 40% throughout the course of this study. It was determined that the optimal passage number for Jurkat cells before transfection was between 2-4, with decreasing efficiencies as cells were cultured for longer periods of time. However, other factors, such as the vendor source of FBS, are also thought to be involved as transfection efficiencies continued to be inconsistent despite the aforementioned changes made.

The final limitation in this study is that the number of biological replicates in our viral transfer studies performed thus far do not support conclusions with robust statistical significance. Given the scale of these experiments, each target could easily be run only once if studying more than one syndecan member at a time. Considering that previous experiments had suggested a role for SDC-1 in viral transfer to HK2 cells, SDC1(-) lines were run in duplicates for transfer studies.

Identification of the receptors that are involved in renal epithelial viral entry may help to explain how the renal tubule cells play an important role in sensing viral infection and initiating an innate immune response that may exacerbate viral infection and local tissue dysfunction. The studies will also help to explain how the renal tissue can serve as a viral reservoir even when plasma viral load has been sufficiently reduced [1-3].

Investigating the viral life cycle in renal tissue may ultimately assist in preventing the onset of HIVAN and further reducing AIDS-related morbidity.

Future directions

Given the potential for cross-reactivity of HSPGs in HIV-1 transfer to HK2 cells, a future assay should consider knocking out multiple members of the syndecan and/or HSPG family in a given experiment. Furthermore, additional methods to assess knockdown, such as Western blots, can be included to account for the levels of total HSPGs expressed at the cell surface and exclude soluble HSPG molecules.

The experimental timeline can also be adjusted to provide a more efficient screening process. For example, multi-target siRNAs or gRNAs may be used to improve individual target knockout efficiencies, which would enable more targets across the HSPG family to be considered at a time.

Furthermore, the transfer assay may be modified through additional staining of target receptors to allow for assessment of cellular-level protein expression that could be directly compared to viral transfer, as opposed to the current population-level expression levels that were obtained separately from the transfer studies. Finally, additional HSPG receptors have yet to be assessed for their role in cell-to-cell viral uptake into HK2 cells, including agrin and perlecan.

LIST OF JOURNAL ABBREVIATIONS

Annu Rev Med	New England Journal of Medicine
Int J Nephrol Renovasc Dis	International Journal of Nephrology and Renovascular Disease
J Am Soc Nephrol	Journal of the American Society of Nephrology
J Virol	Journal of Virology
Matrix Biol	Matrix Biology
Microbes Infect	Microbes and Infection
Mol Biol Cell	Molecular Biology of the Cell
Nat Med	Nature Medicine
Nat Rev Nephrol	Nature Reviews Nephrology
N Engl J Med	New England Journal of Medicine

REFERENCES

1. Cohen, S.D., J.B. Kopp, and P.L. Kimmel, *Kidney Diseases Associated with Human Immunodeficiency Virus Infection*. N Engl J Med, 2017. **377**(24): p. 2363-2374.
2. Diana, N.E. and S. Naicker, *Update on current management of chronic kidney disease in patients with HIV infection*. Int J Nephrol Renovasc Dis, 2016. **9**: p. 223-234.
3. Rosenberg, A.Z., et al., *HIV-associated nephropathies: epidemiology, pathology, mechanisms and treatment*. Nat Rev Nephrol, 2015. **11**(3): p. 150-60.
4. Wyatt, C.M., K. Meliambro, and P.E. Klotman, *Recent progress in HIV-associated nephropathy*. Annu Rev Med, 2012. **63**: p. 147-59.
5. Rao, T.K., et al., *Associated focal and segmental glomerulosclerosis in the acquired immunodeficiency syndrome*. N Engl J Med, 1984. **310**(11): p. 669-73.
6. Bruggeman, L.A., et al., *Renal epithelium is a previously unrecognized site of HIV-1 infection*. J Am Soc Nephrol, 2000. **11**(11): p. 2079-87.
7. Winston, J.A., et al., *Nephropathy and establishment of a renal reservoir of HIV type 1 during primary infection*. N Engl J Med, 2001. **344**(26): p. 1979-84.
8. Marras, D., et al., *Replication and compartmentalization of HIV-1 in kidney epithelium of patients with HIV-associated nephropathy*. Nat Med, 2002. **8**(5): p. 522-6.
9. Canaud, G., et al., *The kidney as a reservoir for HIV-1 after renal transplantation*. J Am Soc Nephrol, 2014. **25**(2): p. 407-19.
10. Blasi, M., et al., *Renal epithelial cells produce and spread HIV-1 via T-cell contact*. AIDS, 2014. **28**(16): p. 2345-53.
11. Phillips, D.M.B., A.S., *Mechanism of HIV Spread from Lymphocytes to Epithelia*. Virology, 1992. **186**: p. 261-73.
12. Hatsukari, I., et al., *DEC-205-mediated internalization of HIV-1 results in the establishment of silent infection in renal tubular cells*. J Am Soc Nephrol, 2007. **18**(3): p. 780-7.
13. Chen, P., et al., *Virological synapses allow HIV-1 uptake and gene expression in renal tubular epithelial cells*. J Am Soc Nephrol, 2011. **22**(3): p. 496-507.

14. Alfsen, A., et al., *HIV-1-infected Blood Mononuclear Cells Form an Integrin- and Agrin-dependent Viral Synapse to Induce Efficient HIV-1 Transcytosis across Epithelial Cell Monolayer*. *Mol Biol Cell*, 2005. **16**(9): p. 4267-79.
15. Christianson, H.C. and M. Belting, *Heparan sulfate proteoglycan as a cell-surface endocytosis receptor*. *Matrix Biol*, 2014. **35**: p. 51-5.
16. Gallay, P., *Syndecans and HIV-1 pathogenesis*. *Microbes Infect*, 2004. **6**(6): p. 617-22.
17. Bobardt, M.D., et al., *Syndecan Captures, Protects and Transmits HIV to T Lymphocytes*. *Immunity*, 2003. **18**: p. 27-39.
18. Shalem, O., et al., *Genome-scale CRISPR-Cas9 knockout screening in human cells*. *Science*, 2014. **343**(6166): p. 84-87.
19. Hubner, W., et al., *Sequence of human immunodeficiency virus type 1 (HIV-1) Gag localization and oligomerization monitored with live confocal imaging of a replication-competent, fluorescently tagged HIV-1*. *J Virol*, 2007. **81**(22): p. 12596-607.
20. Dale, B.M., et al., *Tracking and quantitation of fluorescent HIV during cell-to-cell transmission*. *Methods*, 2011. **53**(1): p. 20-6.

CURRICULUM VITAE

